ChemComm

Check for updates

Self-assembly of M$_4$L$_4$ tetrahedral cages incorporating pendant P=S and P=Se functionalised ligands†

Patrick W. V. Butler, [ID] [a] Paul E. Kruger [ID] [bc] and Jas S. Ward [ID] *[d]
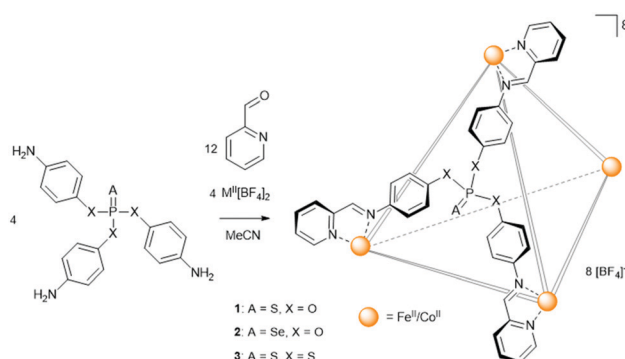
Herein, the synthesis of metal–organic tetrahedral cages featuring flexible thio- and selenophosphate-based ligands is described. The cages were prepared by sub-component self-assembly of A=P(OC$_6$H$_4$NH$_2$-4)$_3$ (A = S, Se) or S=P(SC$_6$H$_4$NH$_2$-4)$_3$, 2-pyridinecarboxaldehyde, and either Fe[BF$_4$]$_2$ or Co[BF$_4$]$_2$. Preliminary host–guest studies into the ability of the pendant P=S and P=Se groups to interact with suitable substrates will be discussed.

The application of metal-directed self-assembly to the formation of discrete architectures has precipitated the development of a myriad of macromolecular metal–organic complexes.[1–4] A subset of these, metal–organic cages, are characterised by containing an internal cavity capable of accommodating substrates in host–guest chemistry.[5–8] By varying the volume and topology of the internal cavity, substrates from simple organic[9–11] and inorganic[12,13] molecules to steroids[14] and fullerenes[15,16] have been successfully encapsulated with those species that most complement the size, shape, bonding and electrostatics of the cavity micro-environment yielding the strongest binding.

The effects of varying the size and shape of the internal cavity are largely intuitive; by contrast, the functionalisation of the micro-environment provides opportunities to investigate more novel host–guest behaviour.[17,18] In this regard, the varied and specific non-bonding interactions of main-group functionalities, including dipole–dipole interactions, chalcogen bonding, and hydrogen bonding, are particularly noteworthy and suggests

the incorporation of these functionalities into supramolecular cages might facilitate stronger and more selective host–guest chemistry.[19,20] Nevertheless, to date main-group functionalised supramolecular cages represent niche structures,[21,22] and especially so when considering those with functionalities based on elements beyond the second row of the periodic table.[23,24] Inspired by work on phosphorus-based porous organic cages (POCs),[25] we have developed a series of metal–organic cages incorporating pendant sulfur and selenium functionalised phosphates.

The basis for the sub-component self-assembly of the cages (Scheme 1) are triamine phosphate pro-ligands, prepared from a mutual tri-substituted phosphite intermediate, subsequently reacted with either elemental sulfur or selenium. The basicity of the amine precluded the direct synthesis of the thio- (**1b**) and seleno-phosphate (**2b**) pro-ligands, however, both were found readily accessible *via* a protecting group strategy (Scheme S1, ESI†). A tetrathiophosphate pro-ligand (**3b**), analogous to **1b**, was similarly prepared with the intention to investigate potential electronic and steric differences compared to the monothiophosphate. To that end, characterisation of **3b** demonstrated a significantly altered phosphate environment. In particular, the ^{31}P NMR resonance of the tetrathiophosphate was identified at 98.1 ppm, considerably further downfield relative to **1b** (57.5 ppm).

[a] *Research School of Chemistry, Australian National University, Acton, Canberra, ACT, Australia*

[b] *School of Physical and Chemical Sciences, University of Canterbury, Private Bag 4800, Christchurch, 8140, New Zealand*

[c] *MacDiarmid Institute for Advanced Materials and Nanotechnology, School of Physical and Chemical Sciences, University of Canterbury, Private Bag 4800, Christchurch 8140, New Zealand*

[d] *Department of Chemistry, Nanoscience Center, University of Jyväskylä, Jyväskylä 40014, Finland. E-mail: james.s.ward@jyu.fi*

Scheme 1 Generalised assembly of the thio- and selenophosphate functionalised M$_4$L$_4$ (M = Fe^{II}, Co^{II}) metal–organic cages.

The M_4L_4 (M = Fe^{II}, Co^{II}) face-capped assemblies were prepared by reacting the phosphate pro-ligands (4 equiv.) in acetonitrile with 2-pyridinecarboxaldehyde (12 equiv.) and either $Fe[BF_4]_2$ or $Co[BF_4]_2$ (4 equiv.).[26] Combining the reagents produced immediate colour changes: the Fe reactions became dark purple, a colour characteristic of a low-spin complex, consistent with the strong-field nature of unsubstituted pyridyl-imine ligands,[27] while the Co assemblies became yellow. The three Fe_4L_4 cages, **1c**, **2c**, and **3c**, and the three Co_4L_4 cages, **1d**, **2d**, and **3d**, were confirmed primarily in solution by HR-ESI MS (Fig. S32–S37, ESI†) with the spectra in each case illustrating a continuous charge series from $[M_4L_4][BF_4]_5^{3+}$ to $[M_4L_4]^{8+}$. Additional analysis of the isotopic manifolds was found to correlate well with simulated data, supporting the assigned identities of the cages.

Suitable X-ray diffraction quality crystals were obtained for two of the assembled supramolecular cages (**1d** and **2d**), and their solid-state structures elucidated. The molecular structure of **1d** (Fig. 1a) revealed the face-capped tetrahedral cage in the orthorhombic $P2_12_12_1$ space group, with only the homochiral diastereomer ($\Lambda\Lambda\Lambda\Lambda$) present in the unit cell. Examining the structure it is apparent the thiophosphate ligands have adopted a 3-*endo*–1-*exo* configuration, wherein three of the pendant P=S groups are positioned inside the internal cavity (*endo*), while the remaining P=S group is positioned outside the cavity (*exo*). This lopsided arrangement contributes to the relative low symmetry of the structure, which presents a crystallographic asymmetric unit cell containing the entire cage, and in which all the ligands are inequivalent.

The separation of the Co^{II} metal nodes of **1d** was found to be between 12.6–14.0 Å, which is consistent with the size of similar M_4L_4 cages reported.[23] The cavity volume, however, could not be calculated using various algorithms, and from the space-filling model (Fig. S3, ESI†) it is clear the cavity is largely occupied by the pendant sulfur atoms of the endohedral ligands. The shortest P=S···S=P distance of 3.620(7) Å is very close to the sum of the

sulfur–sulfur van der Waals radii (3.60 Å), indicative of a favourable interaction between sulfur atoms within the cage. Despite the small cavity in the solid-state, residual electron density was observed within the cage (8.8 e⁻), suggesting solvent or water may be able to access the cavity. This would be consistent with the anticipated lability of the ligands in solution to create dynamically larger windows through which guests may ingress or egress.[28,29]

The three P=S groups *endo*-orientated inside the cage possessed bond lengths within the range 1.917(5)–1.937(7) Å, whilst the final P=S group lying in an *exo*-orientation had a significantly elongated bond length of 2.051(7) Å. The electron density that the *exo* ligand was interacting with could not be satisfactorily modelled, however, the lengthening of the P=S bond is a clear indication that the sulphide groups are not passive in the supramolecular cage.

The molecular structure of **2d** (Fig. 1b) was identified in the centrosymmetric $C2/c$ monoclinic space group. Notably, only the achiral diastereomer ($\Delta\Delta\Lambda\Lambda$) was present in the unit cell. The cage is of similar size to **1d** with Co···Co distances ranging from 12.9–14.9 Å; however, in contrast to the thiophosphate cage, each of the pendant P=Se groups were found to be orientated endohedrally with respect to the cavity. Given the longer P=Se bond length, and the larger atomic size of selenium compared to sulfur, this result infers that the 3-*endo*–1-*exo* configuration observed for **1d** cannot be attributed to steric overcrowding in the interior of the cage, and further reinforces that the *exo* P=S group is orientated to favourably interact with species outside the cage.

The *endo* arrangement of the selenophosphate ligands suggests favourable interactions between the pendant P=Se groups. These interactions, while able to overcome the associated steric congestion, are non-bonding in nature, with neighbouring Se···Se distances of 3.785(3) and 3.811(3) Å beyond the expected length of a formal Se–Se bond (*ca.* 2.39 Å).[30] Furthermore, P=Se bond lengths were found to be slightly shorter in the
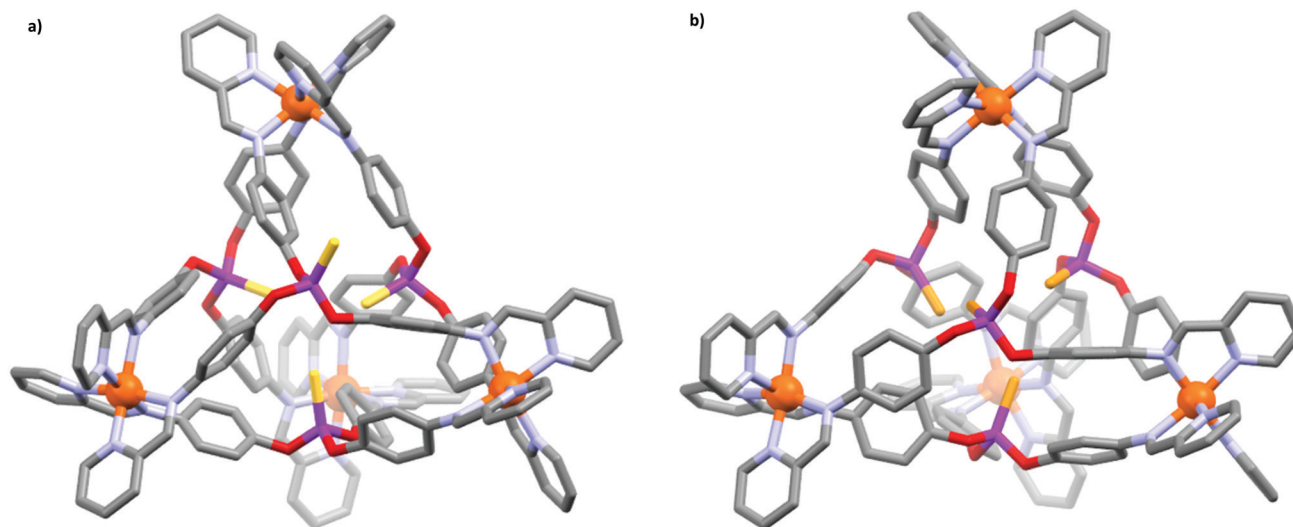

Fig. 1 (a) Molecular structures of the thiophosphate-functionalised Co_4L_4 cage **1d** and (b) the selenophosphate-functionalised Co_4L_4 cage **2d**. The volumes of the Co^{II} atoms (orange) are reduced below the van der Waals radii and the hydrogen atoms, solvent molecules, and counterions omitted for clarity.

assembly (2.045(6)–2.047(5) Å) compared to the parent pro-ligand (*cf.* 2.066(1) Å for **2b**), strongly indicating the P=Se bond is preserved.

The diamagnetic low-spin Fe^{II} assemblies, and to a lesser extent the paramagnetic Co^{II} assemblies, permit further characterisation in solution by NMR analysis. Conventional 1D NMR studies of the assemblies (Fig. S25–S30, ESI†) consistently returned complex spectra with ^{31}P NMR analysis indicating 5–7 inequivalent ligand environments for each cage. The clusters of peaks evident in the ^{1}H NMR spectra are characteristic of equilibria between the anticipated cage diastereomers in solution (*i.e.* homochiral [ΔΔΔΔ/ΛΛΛΛ], heterochiral [ΔΔΔΛ/ΔΛΛΛ] and achiral [ΔΔΛΛ]) in combination with the possible *endo/exo* configurations (of which five unique configurations exist for M$_4$L$_4$ cages). Such complex NMR spectra are common amongst reported non-templated metal–organic cages and are borne out of the lability in solution of the covalent imine bonds and nitrogen-donor coordination bonds combined with the typically small energy differences between the cage isomers.[31,32]

Despite the convoluted spectra, diffusion NMR analysis of the Fe assemblies provided strong evidence of the formation of the expected tetrahedral cages (Fig. 2). Analysis of each of the

cages found a singular slow diffusing species with estimated diffusion constants from 5.37×10^{-10} to 5.55×10^{-10} m^2 s^{-1}, considerably smaller compared to the pro-ligands (13.8×10^{-10} to 14.7×10^{-10} m^2 s^{-1}). Furthermore, using the Stokes–Einstein equation,[33] calculation of the hydrodynamic diameter of the Fe$_4$L$_4$ cages (23.0 to 23.8 Å) correlated well with the average length between the six vertices for the solid-state structure of **2d** (23.6 Å). Considering no other aggregates were observed it can also be concluded that no other thermodynamically stable assemblies resulted from the sub-component self-assembly, and hence the face-capped tetrahedral cages are the sole preferred architecture.

The soft-donor properties of the pendant P=S and P=Se groups inherently inclines the thio- and selenophosphate functionalised cages to host–guest chemistry with similarly soft guest substrates. A preliminary study with a range of heavy metal ions, including Cu^{+}, Hg^{2+}, Pd^{2+} and Au^{+}, complementary to both the reduced size and soft bonding of the cavities, consistently found significant changes in the isomer distributions of the cages as measured by ^{1}H and ^{31}P NMR analysis. For example, combining **3c** with an excess of [Cu(NCMe$_3$)$_4$][BF$_4$] over 24 h and at 50 °C collapsed the isomer distribution to primarily a single ligand environment (Fig. 3). This isomer collapse is indicative of strong interactions with the dopants, and furthermore consistent with the formation of an energetically favourable host–guest complex.[34] Beyond metal ions, the reduced cavity volumes limit the set of potential guests, however, through the modular nature of sub-component self-assembly, options to expand the cages to accommodate larger guests are readily accessible.

In conclusion, we have developed a series of related thio- and seleno-phosphate-functionalised metal–organic cages. The face-capped tetrahedral cages were evidenced in solution by HR-MS and diffusion NMR spectroscopy and in the solid-state by single-crystal X-ray diffraction studies. Notably, the phosphate ligands were found to be capable of independently orientating either endohedrally or exohedrally in reference to the internal cavity. Nascent host–guest studies indicated dominant interactions with soft guest substrates, and investigations are ongoing to develop the host–guest chemistry of these soft donor cages.
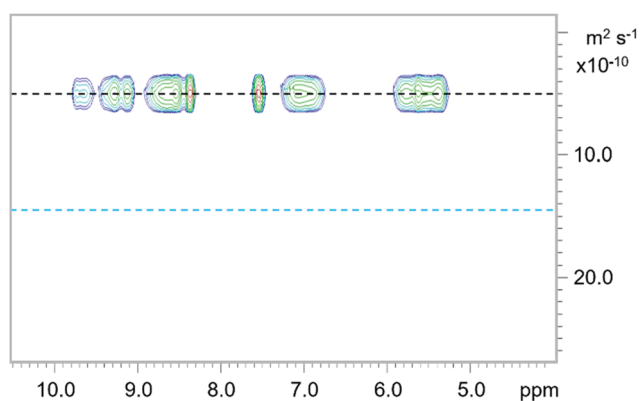

Fig. 2 ^{1}H DOSY plot of the thiophosphate functionalised Fe$_4$L$_4$ assembly **1c**. The diffusion constant of the assembly was estimated at 5.55×10^{-10} m^2 s^{-1} (black line), whereas the corresponding pro-ligand **1b** was estimated at 14.3×10^{-10} m^2 s^{-1} (blue line).
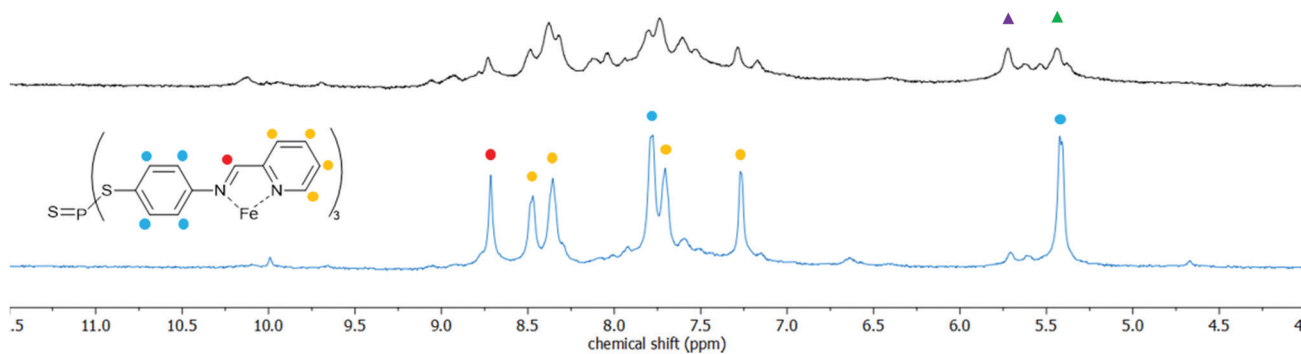

Fig. 3 The ^{1}H NMR spectrum for the tetrathiophosphate-functionalised Fe$_4$L$_4$ **3c** (above) and after mixing with [Cu(NCMe)$_4$][BF$_4$] for 24 h at 50 °C (below). The change in the distribution of the isomers corresponding to the triangle-labelled signals is estimated to be from 1 : 1 (green : purple) before to 10 : 1 after.

Conflicts of interest

There are no conflicts to declare.

Notes and references

1 M. Fujita, *Chem. Soc. Rev.*, 1998, **27**, 417.
2 T. R. Cook and P. J. Stang, *Chem. Rev.*, 2015, **115**, 7001–7045.
3 M. D. Ward, *Chem. Commun.*, 2009, 4487–4499.
4 D. Fujita, Y. Ueda, S. Sato, H. Yokoyama, N. Mizuno, T. Kumasaka and M. Fujita, *Chem*, 2016, **1**, 91–101.
5 A. Ferguson, R. W. Staniland, C. M. Fitchett, M. A. Squire, B. E. Williamson and P. E. Kruger, *Dalton Trans.*, 2014, **43**, 14550–14553.
6 S. J. Dalgarno, N. P. Power and J. L. Atwood, *Coord. Chem. Rev.*, 2008, **252**, 825–841.
7 H. Amouri, C. Desmarets and J. Moussa, *Chem. Rev.*, 2012, **112**, 2015–2041.
8 T. K. Ronson, S. Zarra, S. P. Black and J. R. Nitschke, *Chem. Commun.*, 2013, **49**, 2476–2490.
9 W. Cullen, M. C. Misuraca, C. A. Hunter, N. H. Williams and M. D. Ward, *Nat. Chem.*, 2016, **8**, 231–236.
10 M. D. Pluth, R. G. Bergman and K. N. Raymond, *Acc. Chem. Res.*, 2009, **42**, 1650–1659.
11 G. Szalóki, V. Croué, M. Allain, S. Goeb and M. Sallé, *Chem. Commun.*, 2016, **52**, 10012–10015.
12 R. Custelcean, *Chem. Soc. Rev.*, 2014, **43**, 1813–1824.
13 H. Amouri, L. Mimassi, M. N. Rager, B. E. Mann, C. Guyard-Duhayon and L. Raehm, *Angew. Chem., Int. Ed.*, 2005, **44**, 4543–4546.
14 T. K. Ronson, W. Meng and J. R. Nitschke, *J. Am. Chem. Soc.*, 2017, **139**, 9698–9707.
15 K. Mahata, P. D. Frischmann and F. Würthner, *J. Am. Chem. Soc.*, 2013, **135**, 15656–15661.
16 M. Yamashina, T. Yuki, Y. Sei, M. Akita and M. Yoshizawa, *Chem. – Eur. J.*, 2015, **21**, 4200–4204.
17 P. M. Bogie, L. R. Holloway, C. Ngai, T. F. Miller, D. K. Grewal and R. J. Hooley, *Chem. – Eur. J.*, 2019, **25**, 10232–10238.
18 S. Yi, V. Brega, B. Captain and A. E. Kaifer, *Chem. Commun.*, 2012, **48**, 10295.
19 M. C. Young, L. R. Holloway, A. M. Johnson and R. J. Hooley, *Angew. Chem., Int. Ed.*, 2014, **53**, 9832–9836.
20 R. Custelcean, P. V. Bonnesen, N. C. Duncan, X. Zhang, L. A. Watson, G. Van Berkel, W. B. Parson and B. P. Hay, *J. Am. Chem. Soc.*, 2012, **134**, 8525–8534.
21 M. A. Pitt and D. W. Johnson, *Chem. Soc. Rev.*, 2007, **36**, 1441.
22 H. W. Roesky, I. Haiduc and N. S. Hosmane, *Chem. Rev.*, 2003, **103**, 2579–2596.
23 D. Zhang, T. K. Ronson, J. Mosquera, A. Martinez, L. Guy and J. R. Nitschke, *J. Am. Chem. Soc.*, 2017, **139**, 6574–6577.
24 C. T. McTernan, T. K. Ronson and J. R. Nitschke, *J. Am. Chem. Soc.*, 2019, **141**, 6837–6842.
25 G. Feng, W. Liu, Y. Peng, B. Zhao, W. Huang and Y. Dai, *Chem. Commun.*, 2016, **52**, 9267–9270.
26 A. Ferguson, M. A. Squire, D. Siretanu, D. Mitcov, C. Mathonière, R. Clérac and P. E. Kruger, *Chem. Commun.*, 2013, **49**, 1597.
27 E. C. Volpe, P. T. Wolczanski and E. B. Lobkovsky, *Organometallics*, 2010, **29**, 364–377.
28 T. K. Ronson, A. B. League, L. Gagliardi, C. J. Cramer and J. R. Nitschke, *J. Am. Chem. Soc.*, 2014, **136**, 15615–15624.
29 A. Stephenson, S. P. Argent, T. Riis-Johannessen, I. S. Tidmarsh and M. D. Ward, *J. Am. Chem. Soc.*, 2011, **133**, 858–870.
30 B. W. Tattershall, E. L. Sandham and W. Clegg, *Dalton Trans.*, 1997, 81–87.
31 D. Fiedler, D. Pagliero, J. L. Brumaghim, R. G. Bergman and K. N. Raymond, *Inorg. Chem.*, 2004, **43**, 846–848.
32 A. M. Castilla, W. J. Ramsay and J. R. Nitschke, *Acc. Chem. Res.*, 2014, **47**, 2063–2073.
33 A. Einstein, *Ann. Phys.*, 1905, **322**, 549–560.
34 J. K. Clegg, J. Cremers, A. J. Hogben, B. Breiner, M. M. J. Smulders, J. D. Thoburn and J. R. Nitschke, *Chem. Sci.*, 2013, **4**, 68–76.